

# Self-Assembling Peptides as Cell-Interactive Scaffolds

Elizabeth C. Wu, Shuguang Zhang, and Charlotte A. E. Hauser\*

Cell and tissue engineering therapies for regenerative medicine as well as cell-based assays require an understanding of the interactions between cells with the surrounding microenvironment at the nanoscale. Engineering a cell-interactive scaffold therefore entails control over the nanostructure of the biomaterial. Peptides that are able to self-assemble into 3D scaffolds have emerged as interesting biomaterials for directing cell behavior, with desirable properties such as the capability of tuning the nanostructure by modulating the amino acid composition. Here, an overview of the development of self-assembling peptide hydrogels as functional cell scaffolds is presented, highlighting recent work on incorporating features such as bioactive ligands, growth factor delivery, controlled degradation, and formulation into microgels for defined cell microenvironments.

## 1. Introduction

The ability to culture cells with precise control over cellular behavior and fate can greatly advance the field of tissue engineering and regenerative medicine.<sup>[1]</sup> This requires generating a 3D microenvironment with the appropriate biochemical and mechanical niche for cell regulation.<sup>[2]</sup> In vivo, the microenvironment is comprised of the extracellular matrix (ECM), soluble factors, and neighboring cells.<sup>[3]</sup> While soluble factors can have profound influence on cellular processes, it has also been shown that the insoluble component, or the ECM, plays an integral role in cell patterning, migration, proliferation, and differentiation.<sup>[3,4]</sup> The ECM is comprised of various components such as collagen, fibrin, proteoglycans, and other adhesive proteins, such as laminin and fibronectin.<sup>[1]</sup> It not only provides structural support as a passive scaffold substrate, but also dynamically interacts with the surrounding cells through receptor-mediated signalling, sequestration of growth factors, spatial cues, and transduction of mechanical forces.<sup>[5]</sup> Thus, conventional cell culture in an unnatural 2D environment using a tissue culture plate fails to provide control over cellular processes.<sup>[6]</sup>

Currently, Matrigel, a reconstituted basement membrane derived from mouse sarcoma, is the most widely accepted biomaterial as an ex vivo ECM mimic.<sup>[6,7]</sup> However, its animal origin poses potential problems such as immunogenicity,

high batch to batch variability, and high manufacturing cost.<sup>[8]</sup> Synthetic cell microenvironments are therefore more desirable due to greater control over the physical, chemical, and mechanical properties of the material as well as greater scalability. In this regard, a major challenge is to produce a synthetic biomaterial that either mimics the structure and properties of the ECM, or creates an artificial niche capable of controlling cell behavior in unnatural ways.<sup>[9]</sup> The successful cell scaffold for tissue engineering should therefore possess certain properties for controlling cell behavior, including biocompatibility, appropriate biodegradability, water retention capacity, porosity to allow for cells to grow, and the ability to promote cell proliferation and normal cellular ECM production.<sup>[1]</sup> In addition, synthesis of the scaffold biomaterial must be facile, scalable, reproducible, and cost-effective for successful commercialization.

Hydrogels, 3D polymeric networks capable of holding large amounts of water, have been widely studied as cell scaffolds.<sup>[10]</sup> They have been the material of choice for tissue engineering applications due to their biocompatibility, innate structural similarity to the ECM, and the ability to provide suitable chemical environments.<sup>[9,11]</sup> More specifically, the use of injectable hydrogel formulations in designing cell and tissue engineering therapies have garnered interest as they can improve patient comfort and reduce cost.<sup>[10]</sup> In situ gelling systems for injectable therapies can be made via various methods, including UV-polymerization and self-assembly. Self-assembling systems, characterized by the spontaneous organization of molecules into larger structured arrangements, are particularly attractive because of the ability to engineer materials at the molecular level.<sup>[12,13]</sup> This allows the final structural features of materials at the nanoscale to be tuned by molecular chemistry and assembling environment (such as pH, ionic environment, and temperature).<sup>[14]</sup> Recently, a class of self-assembling hydrogels built from peptides have emerged as promising candidates in biological applications.<sup>[13–19]</sup> Here, we will focus on this class of materials as cell scaffolds.

Peptides are attractive as molecular building blocks as they are inherently biocompatible and biodegradable, can be readily synthesized by standard peptide synthesis protocols, and their structural folding and stability have already been extensively investigated.<sup>[12–14,16,18–20]</sup> Their assembly is highly specific and is regulated by intermolecular interactions governed by non-covalent bonds, including electrostatic, hydrophobic, van der Waals, and hydrogen bonds, as well as aromatic  $\pi$ -stacking.<sup>[18]</sup> Furthermore, the information for self-assembly is encoded in the amino acid sequence, providing the ability to tune and form

Dr. E. C. Wu, Dr. S. Zhang, Dr. C. A. E. Hauser  
Institute of Bioengineering and Nanotechnology  
A\*STAR, 31 Biopolis Way, The Nanos  
138669, Singapore  
E-mail: chauser@ibn.a-star.edu.sg



DOI: 10.1002/adfm.201101905

a diverse range of structural features at the nanoscale level.<sup>[12]</sup> For example, peptides have been used to design diverse architectures such as vesicles, micelles, monolayers, bilayers, fibers, ribbons, and tapes.<sup>[21]</sup> By varying the amino acid sequence, the structural and functional characteristics of the peptide can be modulated, giving rise to “smart biomaterials” that respond to physicochemical triggers such as concentration, pH, light, ionic strength, solvent, and temperature.<sup>[18,21,22]</sup> These characteristics render self-assembling peptides as suitable building blocks for formulating bioactive hydrogels that can mimic the structure and function of the native ECM. In this article, we will describe some of the most recently reported technologies and methods for tailoring biologically active self-assembling scaffolds for improved control of desired cell behavior.

## 2. Types of Self-Assembling Peptide Cell Scaffolds

### 2.1. $\beta$ -Sheet Forming Peptide Hydrogels

The self-assembling peptide EAK16-II, which has a repetitive sequence motif of 16 amino acids (AEAEAKAKAEAEAKAK), was first discovered in baker's yeast by Zhang and co-workers while studying the left-handed Z-DNA binding protein Zuotin.<sup>[17]</sup> They found that the protein adopted a  $\beta$ -sheet configuration by nature of self-complementary ionic interactions and resulted in ordered nanofibers.<sup>[23]</sup> Since then, similar peptides were subsequently designed to form 3D nanofibrous scaffolds capable of supporting cell growth. One classic example is RAD16-II (Ac-RARADADARARADADA-CONH<sub>2</sub>), which consists of alternating hydrophilic and hydrophobic amino acids.<sup>[24]</sup> Similar to EAK16-II, RAD16-II is highly soluble in water and forms a stable  $\beta$ -sheet structure. In addition, through self-complementary ionic interactions, backbone hydrogen bonding, and hydrophobic interactions between the alanine methyl groups, the resulting  $\beta$ -sheets can self-assemble into higher macromolecular structures to form hydrogels with greater than 99% water content. RAD16-II and EAK16-II were both found to be capable of supporting the attachment and growth of a variety of mammalian cells, including fibroblasts and keratinocytes. Interestingly, RGD-binding integrins were not required for cell attachment, and the cells cultured on these peptide hydrogels remained rounded in contrast to cells cultured on conventional tissue culture plates, which spread when attached.<sup>[24]</sup>

Peptides RAD16-I (Ac-RADARADARADARADADA-CONH<sub>2</sub>) and RAD16-II were also evaluated as substrates for neurite outgrowth and synapse formation.<sup>[25]</sup> RAD16-I (now commercially available as PuraMatrix), such as RAD16-II, consists of individual interwoven fibers that are approximately 10–20 nm in diameter (Figure 1). Neurons



**Charlotte A. E. Hauser** received her Diploma in chemistry at the University of Cologne (Germany) and did her Ph.D. studies at the Massachusetts Institute of Technology. She then joined INSERM (Paris, France) and the Max-Planck-Institute of Psychiatry (Munich, Germany). She is currently a Team Leader and Principal

Research Scientist at the Institute of Bioengineering and Nanotechnology (IBN) and an external faculty member of the Medical University of Luebeck, Germany. Prior to joining IBN, she was Founder and Managing Director of Octagene (Martinsried/Munich, Germany). Her research interests include small peptides and peptidomimetics for developing novel biomaterials and therapeutics and the use of G-protein coupled receptors for drug screening and biosensor development.

grown on the scaffold projected extensive neurite outgrowth that followed the contours of the scaffold and were capable of forming active synaptic connections with other neurons at levels similar to those of cells cultured on Matrigel. It was also demonstrated that the peptide scaffolds did not elicit toxicity in rats 5 weeks after implantation. Since these promising initial studies, RAD-16 based scaffolds have been utilized for the

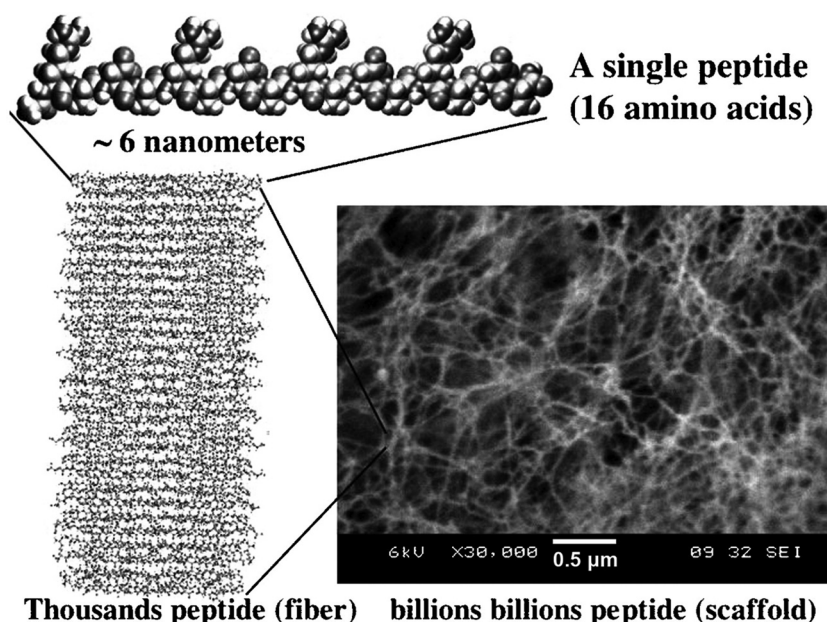


**Figure 1.** Self-assembling peptide RAD16-I nanofiber scaffold hydrogel. Left) Amino acid sequence of RAD16-I and molecular model of a single RAD16-I nanofiber (dimensions are  $\approx 6$  nm long, 1.3 nm wide, and 0.8 nm thick); tens and hundred thousands of individual peptides self-assemble into a nanofiber. Right) SEM image of RAD16-I nanofiber scaffold. Scale bar is 0.5  $\mu$ m or 500 nm. . Reproduced with permission.<sup>[19]</sup> Copyright 2009, Elsevier.

support of a wide range of biological applications, including osteoblast proliferation and differentiation,<sup>[26,27]</sup> axon regeneration,<sup>[28]</sup> and keratinocyte differentiation.<sup>[29]</sup> In addition to applications in tissue regeneration, RAD16-I was recently investigated as a 3D model for ovarian cancer cells, and was found to promote 3D cell adhesion and migration.<sup>[30]</sup> It was found that ovarian cancer cells on the matrix exhibited a higher resistance to anticancer drugs compared to cells grown on a 2D culture plate, allowing for improved anticancer drug screening and in vitro investigation of tumor biology.

KLD12 (Ac-KLDLKLKDLKDL-CONH<sub>2</sub>) is another self-assembling peptide that was designed for the 3D culture of cells.<sup>[31]</sup> Chondrocytes encapsulated in the KLD12 hydrogel maintained their morphology and developed an ECM rich in proteoglycans and type II collagen over a period of 4 weeks, indicative of a stable chondrocyte phenotype. Furthermore, the biocompatibility of KLD12 with rabbit mesenchymal stem cells<sup>[32]</sup> and nucleus pulposus cells<sup>[33]</sup> were also later established, thus demonstrating its potential application in tissue engineering intervertebral discs.

Aggeli and colleagues have also designed another class of  $\beta$ -sheet peptide hydrogels capable of supporting 3D cell culture. They initially showed that Lys $\beta$ -21, whose structure corresponds to residues 41–61 of hen egg white lysozyme, formed hydrogels via triple stranded  $\beta$ -sheets in the  $\beta$ -domain of the protein.<sup>[34]</sup> They further designed a class of peptides including the peptide P<sub>11-4</sub> (QQRFWEFEQQ), in which self-assembly is controlled by pH.<sup>[35]</sup> These peptides can be injected in their monomeric form and triggered to self-assemble in situ by physiological conditions, allowing them to assemble in irregular cavities for the treatment of bone defects, dental hypersensitivity, and dental decay.<sup>[36]</sup> When evaluated for its potential in the treatment of dental caries, it was observed that the peptide was able to induce nucleation of hydroxyapatite de novo and, therefore, is a promising candidate for dental tissue engineering.<sup>[37]</sup>

## 2.2. $\beta$ -Hairpin Forming Peptide Hydrogels

Injectable  $\beta$ -hairpin hydrogel scaffolds based on peptides MAX1 (VKVKVKVK-VDPPT-KVKVKVKV-CONH<sub>2</sub>) and MAX8 (VKVKVKVK-VDPPT-KVEVKVKV-CONH<sub>2</sub>) have been designed by Pochan, Schneider, and co-workers.<sup>[38,39]</sup> MAX1 was shown in early studies to be non-hemolytic toward human red blood cells and capable of supporting the cellular attachment of NIH3T3 cells.<sup>[39]</sup> While MAX1 is not optimal for cell encapsulation due to slow gelation kinetics, MAX8 can encapsulate cells with homogeneous distribution.<sup>[40]</sup> In addition, both MAX1

and MAX8 did not elicit macrophage response in vitro.<sup>[39]</sup> An attractive feature of these peptide hydrogels is the ability of the solid gel to shear-thin and consequently flow upon application of shear stress.<sup>[40]</sup> The solid form and rigidity of the gel can then be recovered upon removal of the external stress. Thus, unlike P<sub>11-4</sub>, these peptides allow for injection as preformed solids. Recently, Yan and co-workers showed that encapsulated MG63 cells remained evenly distributed and viable within the hydrogel during the shear-thin delivery by syringe injection, demonstrating the possibility of using this type of hydrogel as an injectable cell scaffold.<sup>[38]</sup>

## 2.3. $\alpha$ -Helical Peptide Hydrogels

Woolfson and co-workers rationally designed peptides that formed self-assembling fibers (SAFs) based on  $\alpha$ -helical coiled-coils.<sup>[41–43]</sup> The SAFs are composed of two complementary 28-residue peptides containing a heptad sequence repeat,

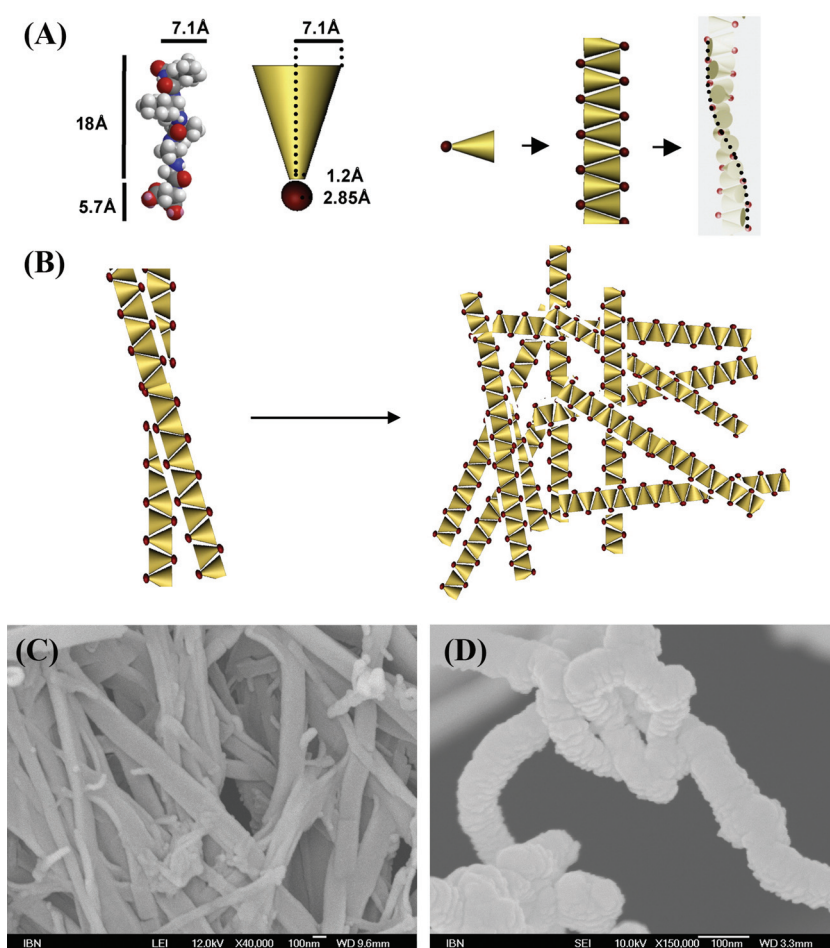


**Figure 2.** A) Schematic representation of the formation of single fibers by stacking of peptide monomers using Ac-LIVAGD (Ac-LD<sub>6</sub>) as a model system. B) Schematic formation of 3D scaffolds or meshes in the form of hydrogels by entangling of individual fibers. C,D) Morphological characterization of the peptide hydrogel scaffolds by field-emission scanning electron microscopy (FESEM). C) Condensed fibers of Ac-LD<sub>6</sub> (L) at a concentration of 15 mg mL<sup>-1</sup> and D) single fibers of Ac-LD<sub>6</sub> (L) at a concentration of 20 mg mL<sup>-1</sup>. Reproduced with permission.<sup>[48]</sup> Copyright 2011, Elsevier.



abcdefg, in which the a and d positions are occupied by isoleucine and leucine, respectively. An advantage of the two component system is the ability to control gelation through the triggering of fiber formation by mixing both components. However, these fibers are highly ordered and precipitated out of solution. To form hydrogelating SAF (hSAF) peptides with over 99% water content, the b, c, and f sites, which are exposed on the surfaces of the coiled-coil assemblies, were replaced with alanine to promote weak hydrophobic interactions between fibrils and glutamine to promote hydrogen bonding.<sup>[44]</sup> To enable the culture of cells, the f position was replaced with tryptophan to stabilize the gel in cell culture media at 37 °C. The resulting hydrogel was found to support bone growth and differentiation of rat adrenal pheochromocytoma cells for sustained culture periods. However, the economic and large-scale production of long peptides for widespread use still remains a challenge.

## 2.4. Ultrashort Aromatic Peptide Hydrogels

Short peptide derivatives have also been shown to self-assemble into  $\beta$ -sheets to form hydrogels that are capable of encapsulating and supporting cell growth.<sup>[45,46]</sup> Zhou and co-workers used Fmoc-diphenylalanine (Fmoc-FF) and Fmoc-RGD as building blocks to form a highly hydrated, stiff (elastic modulus between 4–10 kPa), and nanofibrous hydrogel interlocked by  $\pi$ - $\pi$  stacking interactions of the Fmoc groups.<sup>[45]</sup> The Fmoc-FF/RGD hydrogels were able to promote adhesion of encapsulated dermal fibroblasts through RGD-integrin binding, as replacement of RGD with RGE resulted in rounded cells and poor cell attachment. Recently, Williams and co-workers used Fmoc-trileucine (Fmoc-L<sub>3</sub>) as building blocks to form clear hydrogels comprised of  $\pi\beta$  nanofibrils around 12 nm in diameter and several micrometers long.<sup>[46]</sup> These hydrogels were able to undergo a shear induced gel-sol-gel transition to allow for microinjection. When injected in vivo into zebrafish, it was observed that the hydrogel was confined spatially at the site of injection, demonstrating its stability and potential to treat a targeted diseased area.

## 2.5. Ultrashort Aliphatic Peptide Hydrogels

Recently, Hauser and co-workers have reported a new class of ultrashort peptides that self-assemble into helical fibers in supramolecular structures.<sup>[47]</sup> The characteristic sequence motif of the novel peptide class consists of aliphatic amino acids of decreasing hydrophobicity capped with a hydrophilic head group, such as Ac-LIVAGD (Figure 2a). Surprisingly, these ultrasmall peptides undergo secondary conformational transitions from random coil to  $\alpha$ -helical to cross- $\beta$  structures. The peptide pairs subsequently assemble into fibers and condense into fibrils to form a hydrogel (Figure 2b). The resulting

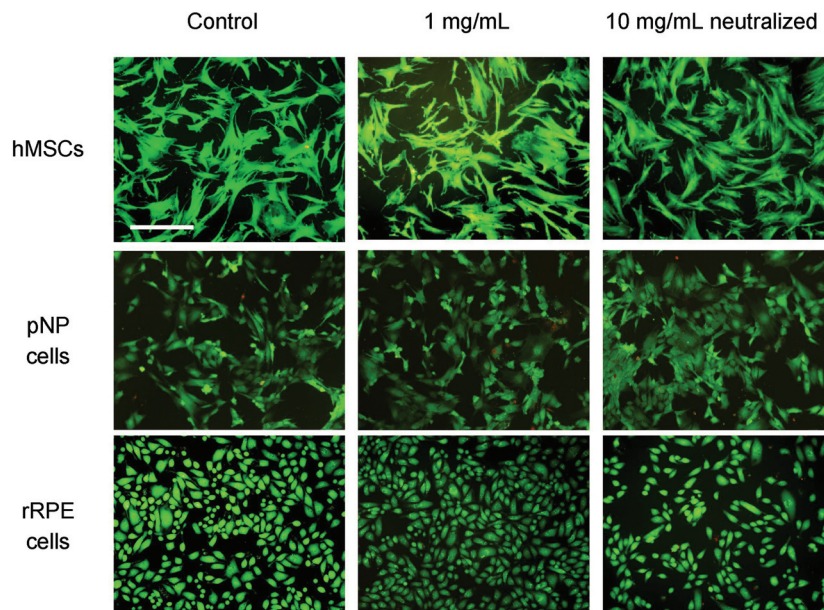


**Figure 3.** Biocompatibility of peptide-derived hydrogels. Viability of human mesenchymal stem cells (hMSCs), porcine nucleus pulposus (pNP) cells, and rabbit retinal pigment epithelial (rRPE) cells after 30 h of exposure to hydrogels derived with different Ac-LD<sub>6</sub> (L) concentrations. Live cells were stained green and dead cells were stained red. Scale bar = 25  $\mu$ m. Reproduced with permission.<sup>[48]</sup> Copyright 2011, Elsevier.

3D hydrogel scaffold is able to entrap up to 99.9% water and resemble collagen fibers in the ECM (Figure 2c).<sup>[47,48]</sup> They were also found to be heat-resistant up to 90 °C and have high and tunable mechanical strength, with the storage modulus ranging between 10<sup>3</sup> to 10<sup>5</sup> Pa. To date, a variety of mammalian primary cells have been successfully cultured on these peptide hydrogels (Figure 3).<sup>[48]</sup> Due to the tunability as well as the facile and decreased cost of synthesis resulting from using ultrashort peptides, this class of peptide hydrogels can serve as attractive biomaterials for applications ranging from injectable biomedical therapies to tissue-engineered scaffolds.

## 2.6. Hybrid Peptide Amphiphiles with Hydrophobic Alkyl Chains

Stupp and co-workers have also created a class of self-assembling peptide amphiphiles in which long alkyl tails attached at the NH<sub>2</sub> or COOH termini of peptides are utilized to impart a hydrophobic region to the molecules.<sup>[49]</sup> These peptide amphiphiles assemble in water into cylindrical micelles and result in nanofibers in which the alkyl tails pack in the center and the active peptide region is displayed on the surface. They further demonstrated the potential in bone tissue engineering by showing the ability of these peptide amphiphiles to direct mineralization of hydroxyapatite along the long axis of the fibers. Peptide amphiphiles containing long alkyl tails have also been evaluated for the ability to support the culture of mesenchymal stem cells (MSC). It was found that the resulting nanofibrous structure was able to enhance the attachment and proliferation of MSCs both on the surface and inside the peptide hydrogel. In addition, differentiation into osteoblasts was demonstrated, indicating that it provides a suitable support for MSC culture.<sup>[50]</sup>

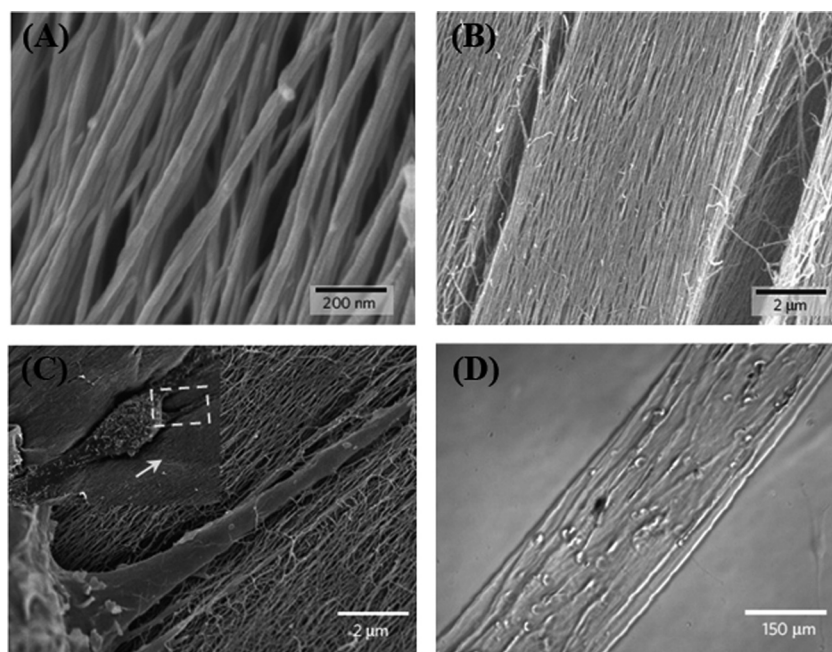


**Figure 4.** A,B) SEM evidence of alignment of nanofiber bundles. Aligned nanofiber bundles in macroscopic strings formed by dragging thermally treated amphiphile solutions onto a  $\text{CaCl}_2$  solution. C) SEM images at different magnifications of a single cell in a string. The inset is the zoom-out view; the arrow indicates the alignment direction. D) Preferential alignment of encapsulated hMSCs along the axis of aligned filaments. Reproduced with permission.<sup>[51]</sup> Copyright 2010, Nature Publishing Group.

More recently, aligned monodomain gels for 3D cell culture have been described using this type of hybrid peptide amphiphile (Figure 4).<sup>[51]</sup> The hydrophilic peptide  $\text{VVVAAEEEE}(\text{COOH})$  was

linked to a  $\text{C}_{16}$  alkyl tail at the N-terminus, and its self-assembly into gels containing nanofibers is triggered by ions that screen the charged amino acid residues. Heating solutions of randomly entangled, isotropic, unscreened molecules aligns the system into long filaments of bundled nanofibers. This unique property was exploited to direct the orientation of MSCs in 3D environments by dispersing the cells in heated and cooled peptide amphiphile solutions followed by manually dragging the solutions onto salty media to form strings with encapsulated cells. Stupp and co-workers are now applying this technology to develop aligned scaffolds to direct cell migration, growth, and spatial cell interconnections for brain, heart, and spinal cord tissue engineering.<sup>[51]</sup>

### 3. Fabrication of Peptide Microgels

For tissue engineering therapies to be effective clinically and treat the targeted disease, large numbers of cells are often required.<sup>[52]</sup> Using conventional tissue culture method, scale-up is costly and difficult due to the limitation of available surface area per volume.<sup>[53]</sup> Microcarriers such as microgels to culture adherent cells in suspension using a bioreactor offer a better alternative for scale-up.<sup>[54]</sup> In addition, microgels that are able to encapsulate cells offer

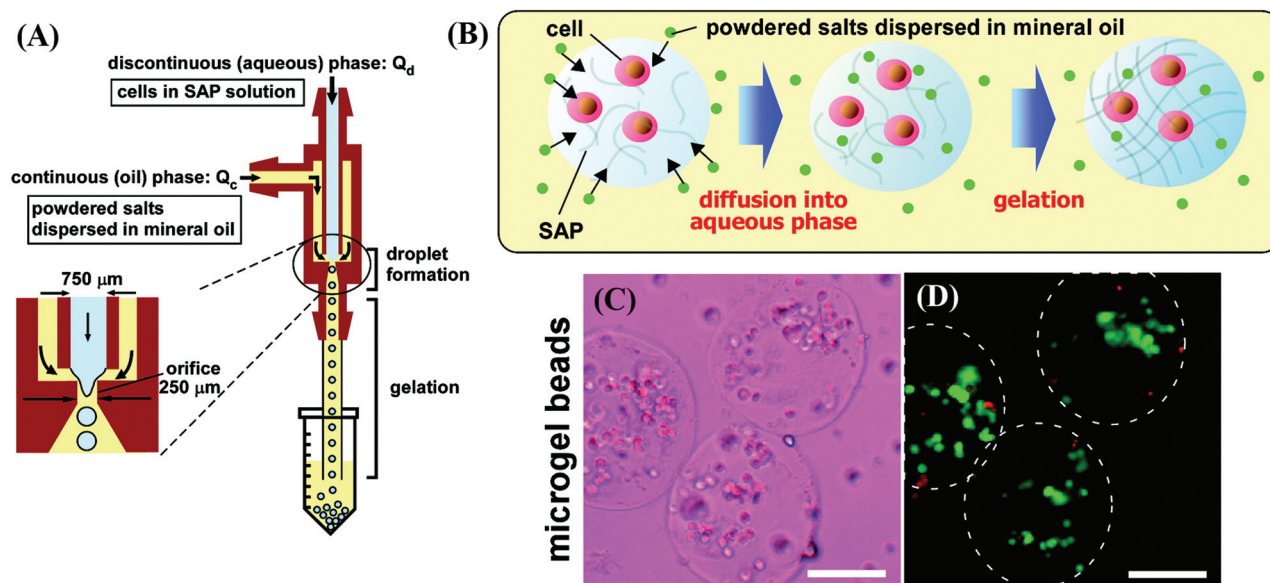


**Figure 5.** A) Schematic illustration of the cell-encapsulating self-assembling peptide microgel formation using an axisymmetric flow-focusing device. The discontinuous (aqueous) phase of the mixed solution of peptides and cells is focused and broken into droplets at the orifice and then collected in the microtube. Powdered salts as a cross-linking agent dispersed into the continuous (oil) phase induce gelation of the peptide solution droplets. B) Mechanism of external gelation of the peptide droplets using the powdered salts. C) Observation of fibroblast cells encapsulated in peptide microgels under bright field. D) Cell viability in the cell-encapsulating peptide microgels with live cells stained green and dead cells stained red. Scale bars = 50  $\mu\text{m}$ . Reproduced with permission.<sup>[56]</sup> Copyright 2009, ACS Publications.



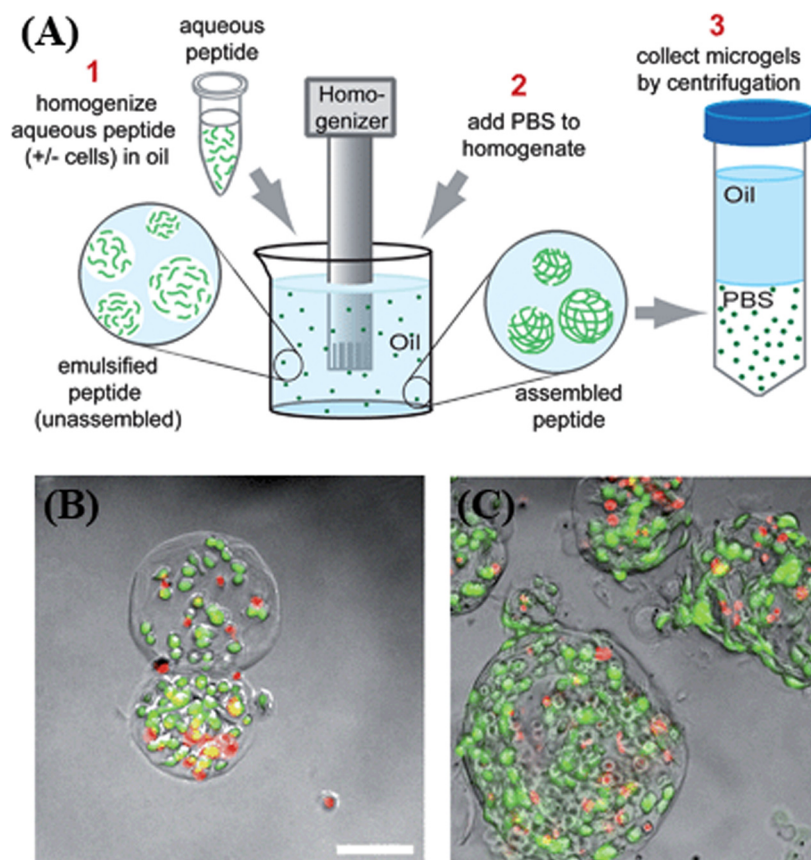


**Figure 6.** A) Schematic for microgel fabrication: A solution of Q11 peptides was added to USP mineral oil and emulsified (1). After formation of a water-in-oil emulsion, a small volume of PBS was added, gelling the peptide in the aqueous phase (2). Microgels were then extracted in excess PBS and collected by centrifugation (3). B,C) The viability of NIH 3T3 cells encapsulated in 30 μm Q11 microgels after B) 1 day and C) 3 days of encapsulation as quantified with calcein/ethidium homodimer staining. Scale bar = 100 μm. Reproduced with permission.<sup>[57]</sup> Copyright 2011, The Royal Society of Chemistry.

added advantages such as the ability to engineer tissues with multiple chemical environments.<sup>[55]</sup> Microgels fabricated from self-assembling peptides have been constructed using various methods, including microfluidics,<sup>[55,56]</sup> microemulsion,<sup>[57]</sup> and electrospray.<sup>[58]</sup>

Tsuda and colleagues fabricated monodisperse cell-encapsulating microgel beads composed of RAD16-I using a microfluidic device.<sup>[56]</sup> An axisymmetric flow-focusing device (AFFD) was designed such that a channel containing the mixture of cell suspension with the peptide can be introduced into another channel containing an oil mixture (Figure 5a). Gelation was induced by the introduction of finely powdered salts and the diameter of the microgels was controlled by flow rate. After 3 days in culture, it was observed that the encapsulated fibroblast cells migrated and formed cell–cell contacts within the gel, indicating the gels are able to facilitate diffusion of nutrients and support cell proliferation (Figure 5b,c). Furthermore, this system is compatible for culture of cells on the outer surface of the gel.

The  $\beta$ -sheet fibrillizing peptide Q11 (Ac-QQKFQFQFEQQ-Am) has also been used for forming cell encapsulating microgels by ionic strength changes in combination with

emulsion processing (Figure 6a) by Tian and co-workers.<sup>[57]</sup> Solutions of the peptide were added to oil, and by adding phosphate buffered saline (PBS), the aqueous peptide could be gelled. The resulting peptide hydrogels could subsequently be collected by rinsing with excess PBS. Although the size of the microgels could be tuned by varying the blade speed of the homogenizer, it cannot be as precisely tuned as by microfluidic methods. However, the simplicity of fabrication using this method facilitates ease of scale up. This process was also found to be suitable for cell encapsulation, with about 80% cell viability immediately after processing and the maintenance of this viability for at least 3 days in culture (Figure 6b). In addition, significant growth was observed for encapsulated 3T3 cells, suggesting the microgels provided a suitable microenvironment for their culture.

The class of peptide amphiphiles developed by the Stupp laboratory has also been demonstrated to form microcapsules.<sup>[58]</sup> They built a spray-based device that enables production of microliter droplets of biopolymer solution such as alginate. The microdroplets were then directly ejected to the peptide amphiphile aqueous solution and self-assembly occurred on the millisecond timescale. Gelation occurred by introduction of  $\text{Ca}^{2+}$  ions during or after microcapsule formation. This platform was modified to encapsulate and release proteins and macromolecules by incorporating molecules such as bovine serum albumin (BSA) into the spray solution. Successful encapsulation of dextrans and BSA was observed and release of

the molecules occurred over a period of 24 h. As these microcapsules have a high surface area due to its fibrous surface and allow for the delivery of various proteins and macromolecules, they have potential for cell-mimetic functions.

## 4. Biofunctionalization of Peptide Hydrogels

### 4.1. Incorporation of Bioactive Ligands

The nanoscale presentation of biologically relevant molecular signals, such as bioactive peptide ligands, can be used to direct cell behavior.<sup>[59]</sup> In particular, recent findings have demonstrated that the microenvironment directly influences cell lineage specification. Therefore, bioactive molecules that are able to promote cell adhesion, migration, proliferation, or differentiation have been incorporated into self-assembling peptide hydrogels to create niche environments tailored for specific cell types.

For example, biologically active motifs have been incorporated into peptide amphiphiles by Silva and co-workers for

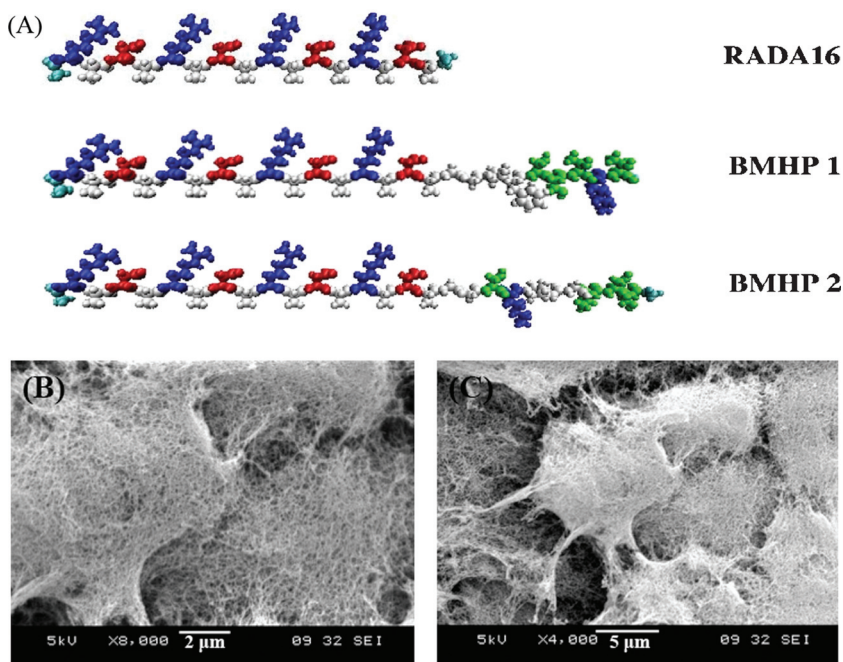


**Figure 7.** A) Molecular models of RAD16-I, RAD16-bone marrow homing peptide 1 (BMHP1), RAD16-bone marrow homing peptide 2 (BMHP2). The BMHP1 and BMHP2 motifs were directly extended from RAD16-I with two glycine spacers and are composed of a lysine (blue), serine and threonine (green), and different hydrophobic (white) residues. B,C) Cluster of mouse adult neural stem cells fully embedded in the self-assembling peptide nanofiber scaffold. The scales of the peptide nanofibers are on a similar scale as the native ECM that is made and secreted by cells. These images show that fiber dimensions between the peptide scaffold matrix and ECM are indistinguishable. This illustrates the importance of nanoscale, rather than microscale, of most other biopolymeric materials. Such 3D cell clusters are nearly impossible to form in the 2D culture systems or microfiber biomaterials. These biologically functionalized scaffolds fully promote cell-matrix interactions. Reproduced from ref. [63].

designing improved cell-interactive scaffolds.<sup>[60]</sup> In early studies, IKVAV (an active sequence of laminin) was incorporated to the previously described peptide amphiphiles to promote neurite sprouting and direct neurite growth of neural progenitor cells (NPCs). The resulting nanofibers formed from the peptide amphiphiles presented the incorporated epitopes in 3D to the entrapped cells. Using the IKVAV-peptide amphiphile scaffold, rapid differentiation of NPCs was induced while the development of astrocytes was inhibited, allowing selective differentiation. Since then, various other bioactive motifs have also been incorporated to enhance potential in regenerative medicine, including a transforming growth factor (TGF) binding domain for articular cartilage regeneration.<sup>[61]</sup> In vitro, it was shown that the matrix was able to support human MSC viability and chondrogenic differentiation and can retain TGFβ-1 within the gels. Furthermore, it was shown that the healing of chondral defects can be accelerated with this system in vivo. More recently, peptide amphiphiles with biomimetic elements to induce hydroxyapatite nucleation was used to promote bone regeneration in a rat femoral critical-size defect.<sup>[62]</sup>

Bioactive sequences from various types of ECM proteins such as collagen, laminin, and fibronectin as well as osteopontin, osteogenic, and bone marrow homing peptides have also been appended to RAD16-I and evaluated for their effect on mouse adult neural stem cells.<sup>[63]</sup> It was found that two of the scaffolds

functionalized with a bone marrow homing peptide enhanced cell survival and promoted differentiation towards neuronal and glial cells without the addition of soluble growth factors and neurotrophic factors (Figure 7). Variations of bone marrow homing peptide 1 (BMHP1) appended to RAD16-I were later systematically studied for their effect on self-assembly and biomechanical properties.<sup>[64]</sup> It was discovered that a majority of the peptides demonstrated self-healing capability, allowing them to recover their stiffness after rupture. In addition to promoting neural stem cell proliferation and differentiation in vitro, the peptide hydrogels showed good short-term in vivo biocompatibility when injected into the spinal cord of rats<sup>[64]</sup> and were later shown to ameliorate the locomotor recovery of rats.<sup>[40]</sup> Following these studies, IKVAV was also appended to RAD16-I to improve rat neural stem cell proliferation and migration into the nanofiber matrix.<sup>[65]</sup> Furthermore, RAD16-I hydrogels have also been functionalized with bioactive ligands to enhance the proliferation, differentiation, and 3D migration of osteoblasts and human periodontal ligament fibroblasts.<sup>[26,66]</sup>

## 4.2. Delivery of Proteins and Hormones

### 4.2.1. Cardiac Tissue Engineering

As mentioned previously, soluble molecules such as growth factors are an important component in the cellular microenvironment, and thus the ability to achieve controlled release of soluble factors can aid in obtaining the desired cell behavior.<sup>[2,67]</sup> This strategy has been applied in improving the function of self-assembling hydrogels as cell scaffolds, including for applications in cardiac tissue engineering.<sup>[68–70]</sup> Cardiac repair through injection of cells has been hampered by poor cell engraftment, survival, and differentiation.<sup>[71]</sup> To address this issue, insulin-like growth factor 1 (IGF-1) was biotinylated and bound to biotinylated RAD16-II through streptavidin, as IGF-1 has been shown to be a potent cardiomyocyte growth and survival factor.<sup>[68]</sup> It was found that biotinylation of IGF-1 did not affect its bioactivity and that tethered IGF-1 peptides promoted cardiomyocyte proliferation in vitro. When studied in vivo, more prolonged delivery of IGF-1 was achieved from tethered IGF-1 peptides than from free IGF-1 or non-biotinylated peptides embedded with IGF-1. It was conjectured that cells were able to secrete proteases to degrade the gel and release tethered IGF-1 in a sustained manner. In addition, implanted cells delivered with tethered IGF-1 peptides improved the therapeutic outcome compared to implanted cells alone.

In more recent work, dual delivery of growth factors including basic fibroblast growth factor (FGF2), vascular endothelial growth factor (VEGF), and platelet derived growth factor (PDGF) was demonstrated to improve the function of



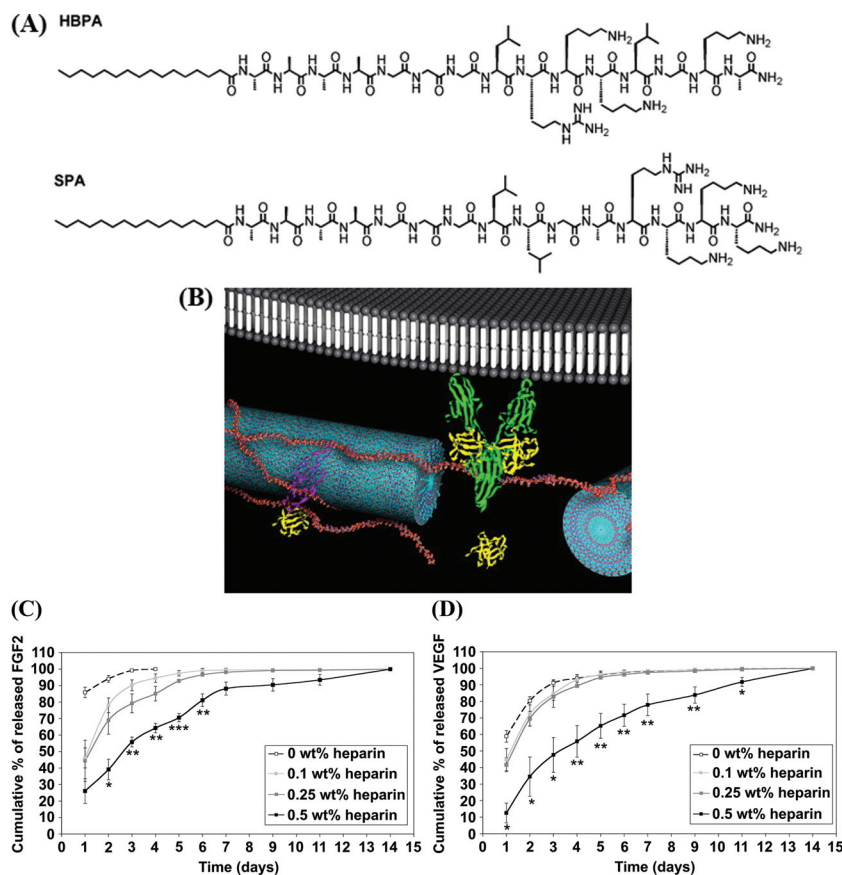


**Figure 8.** A) Molecular structure of HBPA. B) Schematic representation of heparin-nucleated HBPA nanofibers interacting with GF and receptors. The HBPA nanofibers (blue) are shown with adsorbed heparin chains on them (red). Heparin is known to bind and activate VEGF (purple), FGF-2 (yellow), and FGF receptor (green). Reproduced with permission.<sup>[73]</sup> Copyright 2008, Elsevier. Cumulative release of C) FGF-2 and D) VEGF from membranes self-assembled from 2 wt% HBPA and 1 wt% HA with varying concentrations of heparin. Statistical significance is only shown for 0.5 wt% heparin against all other groups (\* $P < 0.05$ , \*\* $P < 0.01$ , \*\*\* $P < 0.001$ ). Reproduced with permission.<sup>[70]</sup> Copyright 2011, Elsevier.

the peptide matrix. In one report by the Stupp laboratory, FGF2 and VEGF were bound to heparin binding peptide amphiphile (HBPA) nanofibers to promote angiogenesis (Figure 8)<sup>[70,72,73]</sup> The HBPA nanofiber gels were demonstrated to persist in vivo for up to 30 days and exhibited excellent biocompatibility.<sup>[74]</sup> After incorporation of FGF2 and VEGF, the HBPA nanofiber provided sustained release of the growth factors for 14 days in media. When evaluated for their angiogenic efficiency in vivo, HBPA nanofibers loaded with the growth factors stimulated a more rapid angiogenesis than HBPA nanofibers without the growth factors. Similarly, the delivery of PDGF and FGF-2 using RAD16-II peptides improved cardiac function, led to stable vessel formation, and reduced infarct size compared to peptide scaffold controls without the growth factors.<sup>[69]</sup>

#### 4.2.2. Cartilage and Other Tissue Engineering

For cartilage tissue engineering applications, self-assembling peptide (KLDL)<sub>3</sub> was modified by Kopesky and co-workers to deliver transforming growth factor  $\beta$ -1 (TGF- $\beta$ 1), which has been used to promote chondrogenesis of bone marrow

derived stromal cells (BMSCs) in vitro.<sup>[75]</sup> BMSC-seeded peptide hydrogels contained either tethered TGF- $\beta$ 1 (Teth-TGF) or physically adsorbed TGF- $\beta$ 1 (Ads-TGF). Interestingly, Ads-TGF stimulated chondrogenesis of BMSCs and production of full-length aggrecan whereas Teth-TGF did not. Potential explanations include Teth-TGF ligand entrapment preventing interaction between the ligand and cell surface receptors. The delivery duration of growth factors for chondrogenesis promotion will need to be further evaluated.

In another example, delivery of Sonic hedgehog (SHH) using aligned peptide amphiphile nanofibers was used to improve the regeneration of the cavernous nerve, which provides innervation to the penis.<sup>[76]</sup> Aligned monodomain peptide gels were used to provide directional guidance to regenerating axons as well as to deliver proteins directionally for sustained periods. Using this strategy, the peptide gels were able to deliver SHH in a manner that did not elicit an immune response. Furthermore, delivery of SHH via peptide gels promoted cavernous nerve regeneration and suppressed penile apoptosis. This methodology may be applied to the regeneration of other peripheral nerves in which SHH is required for function. Therefore, incorporating the ability to controllably deliver biologically relevant molecules may improve and broaden the applications of self-assembling peptide hydrogels.

#### 4.3. Incorporation of Cleavable Sequences for Controlled Degradation

The ability to allow for matrix remodeling is an important feature in the control and guidance of cell behavior for tissue regeneration. Matrices encapsulating cells should allow for cell-mediated degradation such that cells are able to create pathways to spread, proliferate, migrate, and remodel into interconnected tissues for optimal material properties.<sup>[77]</sup> As such, there has been interest on controlling the degradation of self-assembling peptide hydrogels and rendering them susceptible to degradation by ECM proteases for continuous matrix remodeling. For example, a matrix metalloproteinase (MMP)-labile sequence (PVGLIG) was inserted in between RADA units with varying lengths.<sup>[78]</sup> It was found that inserting PVGLIG directly inhibited assembly and resulted in a non-gellable peptide due to disruption of  $\beta$ -sheet assembly. Thus, there must be sufficient RADA units to overcome the effect of inserting PVGLIG, which was hypothesized to form a random coil region (Figure 9). Optimal self-assembling and mechanical properties was observed when three repeats of RADA flanked the MMP-labile sequence. After exposure to MMP-2 for 24 h, enzymatic cleavage occurred for gels containing PVGLIG while control peptide gels without PVGLIG showed



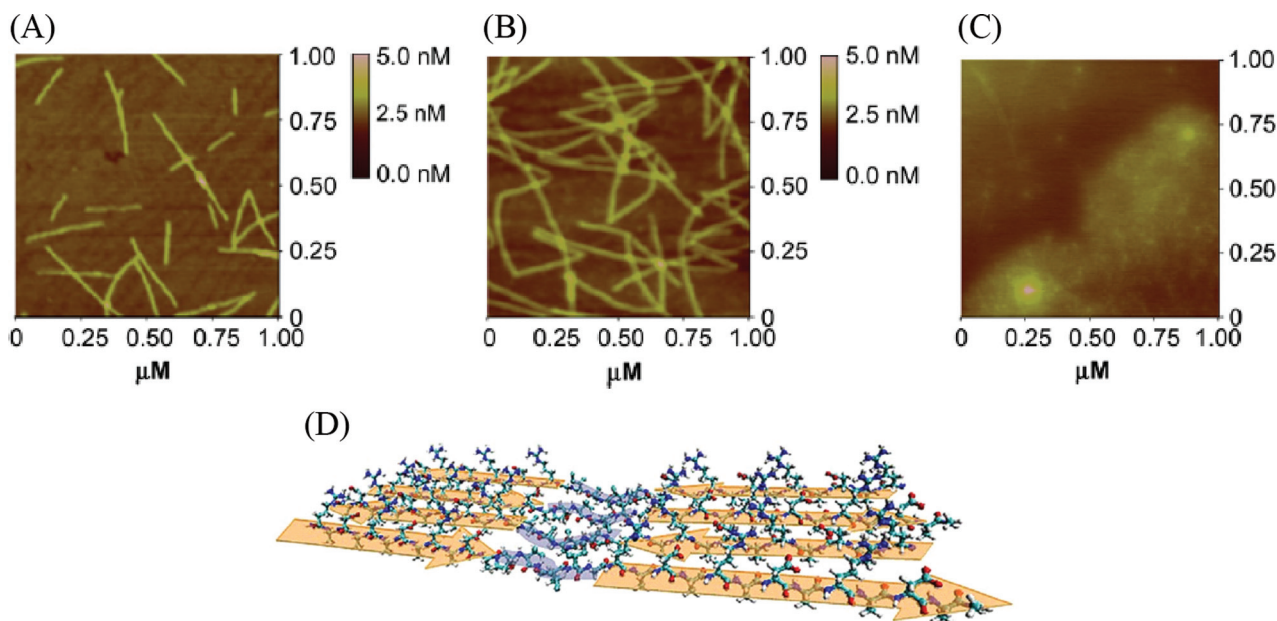


**Figure 9.** Atomic force microscopy (AFM) images of the peptides A)  $(\text{RADA})_3\text{PVGLIG}(\text{RADA})_3$ , B)  $(\text{RADA})_4$ , and C)  $(\text{RADA})_2\text{PVGLIG}(\text{RADA})_2$ . The first two peptides self-assemble into nanofibers in water while the last one is incapable of fiber formation. A  $1\ \mu\text{m} \times 1\ \mu\text{m}$  field is shown for each peptide. The gradient scale bars next to each frame spans a Z (height) range from 0 to 5.0 nm (A and B) and 0 to 8 nm (C). D) Proposed  $\beta$ -sheet assembling model for [3,3] peptide, where peptide chains align in antiparallel directions with a random coil region of PVGLIF (blue) between RADA assemblies via energetically favorable interactions (arrows). A single sheet with four  $\beta$ -strands is shown for clarity. Reproduced with permission.<sup>[78]</sup> Copyright 2011, Elsevier.

an insignificant amount of cleavage. Additionally, digestion was localized to the surface of the gel, mimicking proteolysis, and ECM remodeling *in vivo*. More recently, PVGLIG was also incorporated into shorter self-assembling peptides to accelerate fibroblast migration.<sup>[79]</sup>

Another class of self-assembling multidomain peptides, designed by Galler and co-workers, has recently been modified to incorporate the MMP-2 specific cleavage site LRG.<sup>[80]</sup> This class of peptides contains a modular ABA block motif such as  $\text{K}_2(\text{SL})_6\text{K}_2$ , in which the amphiphilic B block drives self-assembly and the electrostatically charged A blocks control the self-assembly conditions. The incorporation of a MMP-2 cleavage site in the central block motif allowed for proteolytic degradation of the hydrogel in the presence of collagenase IV and promoted increased cell spreading and migration into the hydrogel matrix compared to control. In addition, these peptides are able to undergo shear thinning and recovery of nearly 100% of their elastic modulus upon removal of the shear force and thus can be used as an injectable system.<sup>[81]</sup>

A MMP-2 cleavable site composed of GTAGLIGQ has also been incorporated into peptide amphiphiles to closer mimic the ECM.<sup>[77,82]</sup> This peptide self-assembles upon addition of divalent cations, which shield the repulsive negative charges present. When incubated in type IV collagenase, the gels lost 50% of their weight within 1 week and were completely degraded after 1 month. TEM imaging revealed that the nanofibers (7–8 nm diameter and several micrometers in length) initially present turned into fibrillar aggregates or multistranded ribbons, indicating the enzyme cleavable sites result in defects in fiber packing. Pulp cells encapsulated in peptide

hydrogels with the MMP-2 cleavable site were able to spread and elongate on the fiber network, whereas cells remained rounded in control gels. This suggests that cells were able to secrete enzymes to create a pathway and remodel the network within the hydrogel.

Additionally, controlled degradation of self-assembling  $\beta$ -hairpin peptide hydrogels specific to MMP-13 was recently reported.<sup>[83]</sup> Giano and co-workers designed a new group of degrading peptides, which are composed of 20 amino acid residues that incorporate MMP-13 specific cleavage sites with varying MMP-13 susceptibility. This class of peptides can be triggered to self-assemble by increasing ionic strength to screen positive charges present on the lysine side chains. PTG-XKV, where X is variable, was appended to the C-terminus of the peptide to impart MMP-13 susceptibility. Over a period of 14 days, degradation of the gels was found to be specific to MMP-13, with minimal cleavage by MMP-3. In addition, migration assays with SW1353 cells induced to express MMP-13 revealed that the cell migration rate corresponded with the rate of gel degradation. Thus these gels show potential as an ECM mimic to allow for matrix remodeling during the repair of damaged tissues with elevated levels of MMP-13.

## 5. Hybrid Systems

Self-assembling peptides have also been utilized to improve the biological properties of otherwise weakly bioactive scaffolds.<sup>[84–87]</sup> Ti-6Al-4V for example, is a promising metallic scaffold candidate for orthopedic implants, as it can be foamed to achieve a porosity of approximately 50%.<sup>[84,88]</sup> The foaming

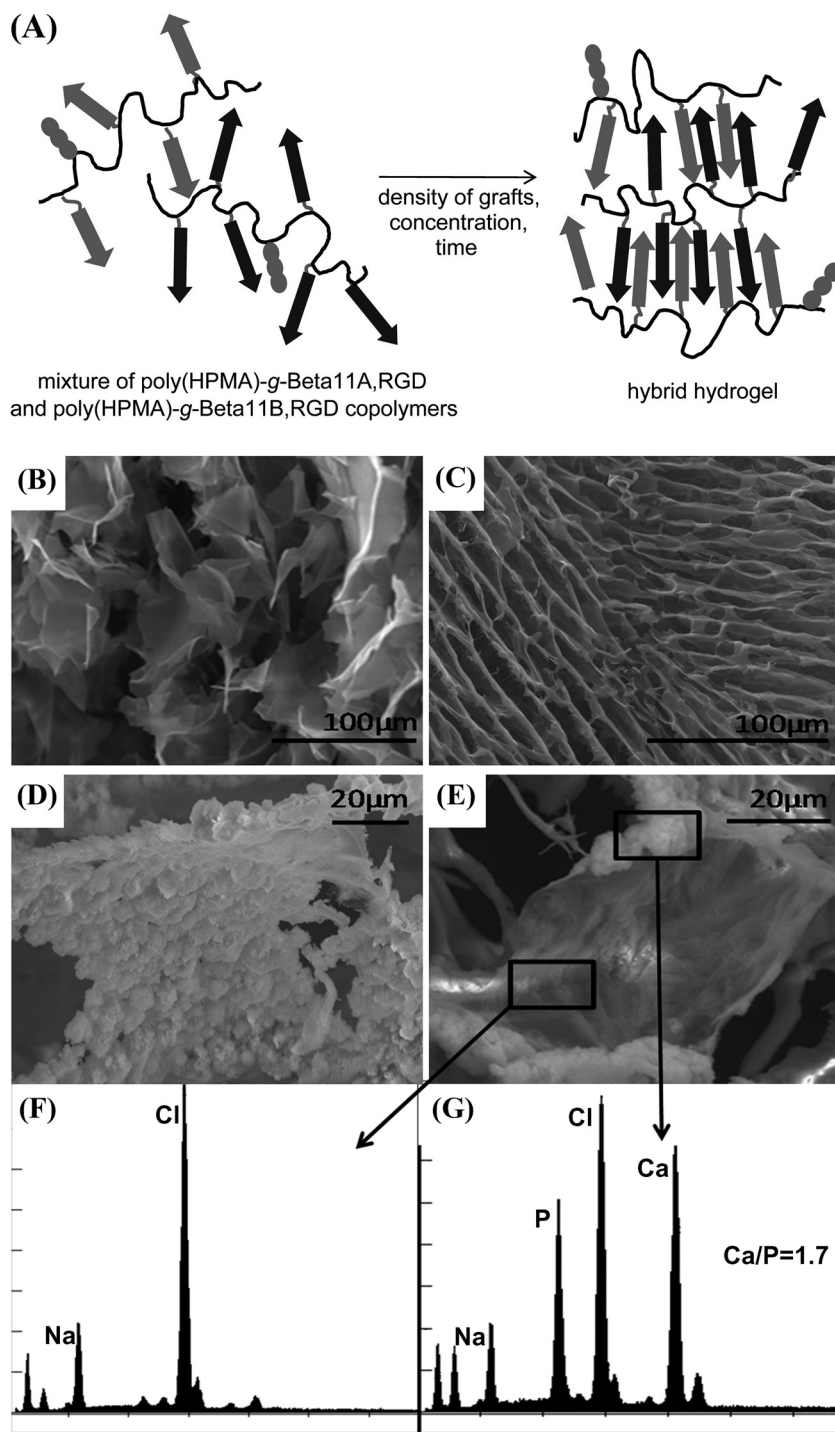


**Figure 10.** A) Proposed model of hybrid hydrogel formation from self-assembled poly(HPMA)-g- $\beta$ -sheet complementary copolymers. SEM images of B) Beta11A:Beta11B, and C) poly(HPMA)-g-Beta11A,RGD:poly(HPMA)-g-Beta11B,RGD lyophilized hydrogels before mineralization. SEM images of HA crystals deposited on the surface of poly(HPMA)-g-Beta11A,RGD:poly(HPMA)-g-Beta11B,RGD (D,E). EDS spectra corresponding to minerals F) inside and G) on the edge of the pores. Ca/P = 1.67 in HA or carbonated HA. Reproduced with permission.<sup>[86]</sup> Copyright 2011, Elsevier.

results in a reduction of the Young's modulus to obtain a greater similarity to bone in stiffness as well as to allow for possible cell ingrowth. However, Ti-6Al-4V foams do not have the ability

to directly guide cell behavior and promote bone formation. To overcome this limitation, Sargeant and colleagues filled the Ti-6Al-4V foam with a peptide amphiphile nanofiber matrix that self-assembles in situ within the foam.<sup>[84]</sup> This strategy allowed for the encapsulation of pre-osteoblastic cells within the matrix. In addition, the incorporation of a phosphoserine residue in the peptide amphiphile induced nucleation of calcium phosphate, which enhances osteoconductive properties. When tested in vivo using a rat femoral model, new and highly mineralized bone with the same structure as cortical bone was observed adjacent to as well as inside the implant, indicating osteoconduction.

Tissue engineering of bone using a hybrid scaffold composed of self-assembling peptides and poly(2-hydroxyethyl methacrylate) (poly(HEMA)) has also been investigated.<sup>[86]</sup> Poly(HEMA) has been shown to be able to support the growth of HA crystals while peptides in  $\beta$ -sheet conformation can nucleate the growth of HA. Therefore, complementary  $\beta$ -sheet peptides Beta11A and Beta11B, designed after Aggeli's model of P11-3 and P11-4, were grafted with poly(HPMA). Fibrils with hierarchic  $\beta$ -sheet structures were formed upon self-assembly and the  $\beta$ -sheet template of the hybrid hydrogel was able to promote mineralization of HA-like crystals (Figure 10). In addition, preosteoblast cells were encapsulated inside the hydrogels and remained viable after 1 week in culture. However, the hybrid scaffold is not strong enough to serve as a bone grafting material, but may serve to initially control mineralization and cell distribution.

Soft tissue engineering may also benefit from hybrid hydrogel scaffolds, as demonstrated by the self-assembling peptide EFK8 (Ac-KFEFKFEF-CONH<sub>2</sub>) used in combination with poloxamer 507 (PO) as a biomaterial.<sup>[85]</sup> PO is a thermoreversible scaffold that can facilitate tissue formation and has promising drug release characteristics. However, a drawback of this material is its non-ionic nature, which results in uneven distribution and aggregation of cells. On the other hand, self-assembling peptide based hydrogels have suffered from lower mechanical strength compared to other hydrogel systems. By combining EFK8 with PO, the hybrid hydrogel resulted in improved mechanical strength and bioactivity compared to each individual component taken alone. Human adipose derived MSCs were able to disburse evenly throughout the hybrid gel and maintained cell viability. In addition, adipogenic differentiation was achieved in vivo when the hybrid hydrogel was implanted in nude mice.



Electrospinning has recently been applied for developing hybrid peptide-polymer systems.<sup>[87,89]</sup> In one example, a hybrid system composed of electrospun polycaprolactone and peptide amphiphiles for vascular tissue engineering was synthesized.<sup>[87]</sup> Electrospinning was used to deposit nanofibers in a rotating mandrel to create a tubular structure and the peptide amphiphiles were used to confer bioactivity. Nitric oxide (NO) donating residues were incorporated into the peptide amphiphile as NO is an important regulator in the vascular environment. This hybrid matrix was found to inhibit smooth muscle cell adhesion as well as to promote endothelial cell adhesion, which is critical in re-endothelialization and prevention of restenosis. In addition, platelet adhesion was also reduced compared to collagen scaffolds, which can potentially be exploited to prevent thrombosis. These findings indicate that hybrid matrices have great potential as biomimetic implants by achieving improved properties compared to individual components.

## 6. Conclusions and Future Outlook

We have highlighted the development of self-assembling peptide hydrogels as cell scaffolds to control cell adhesion, proliferation, migration, and differentiation. With regards to the properties of an ideal scaffold, it has already been demonstrated that the versatility of self-assembling peptides is spurring their advancement to meet these requirements. As discussed, using amino acids as building blocks, self-assembling peptides have innate biocompatibility and biodegradability.<sup>[14]</sup> Their in situ assembly also allows for easy incorporation of cells during formation and their possibility as minimally invasive injectable therapies.<sup>[90]</sup> Since each tissue differs morphologically and physiologically, their respective ECM also differs significantly.<sup>[1]</sup> Therefore, the ability to tailor each biomaterial to create the appropriate biochemical and mechanical microenvironment for a particular application will offer greater control over the desired cellular behavior. In working toward that goal, self-assembling peptides have been decorated with various biologically active ligands and cleavable sequences, modified to release biologically active molecules such as growth factors, and formulated into microgels for the possibility of creating distinct microenvironments within the same tissue construct.

Despite these advances, a greater understanding of the structural design and self-assembly process is needed to further advance their application in regenerative medicine. For example, an advantage of  $\beta$ -structure self-assembling peptides is the ease in which bioactive motifs and cleavable sequences for degradation can be incorporated without disruption, due to the strong forces that govern self-assembly. However, modifying  $\alpha$ -helical based self-assembling peptides without disrupting the self-assembly process poses greater difficulties, but non-covalent functionalization with peptide tags offers a possible route to rendering this class of peptide hydrogels bioactive.<sup>[91,92]</sup> It is also still a challenge to be able to design various molecules that assemble in a predictive manner to a wide range of desired structures, although rational design of supramolecular structures are steps toward that direction.<sup>[93,94]</sup> In addition, while the use of self-assembling peptides have largely been limited to soft tissue engineering, the development of hybrid systems

may offer an interesting avenue in expanding their application. Finally, solid-state synthesis of peptides may be efficient for small scale production, but its scale up can be expensive.<sup>[95]</sup> Therefore, to generate a commercially viable product, the cost of production needs to be reduced. Using ultrashort peptide sequences for self-assembly and synthesizing the peptides using recombinant technology may offer possible solutions.

In summary, the full potential of self-assembling peptides for cell and tissue engineering has yet to be fully realized, and their versatility in creating tailored biologically active structures warrants further investigation.

## Acknowledgements

The authors thank Dr. Yihua Eva Loo, Dr. Wei Yang Seow, Archana Mishra, and Anupama Lakshmanan for their help with proofreading. This work was supported by the Institute of Bioengineering and Nanotechnology (Biomedical Research Council, Agency for Science, Technology and Research (A\*STAR), Singapore).

Received: August 14, 2011

Published online: December 21, 2011

- [1] R. C. Dutta, A. K. Dutta, *Biotechnol. Adv.* **2009**, *27*, 334.
- [2] D. E. Discher, D. J. Mooney, P. W. Zandstra, *Science* **2009**, *324*, 1673.
- [3] R. Ayala, C. Zhang, D. Yang, Y. Hwang, A. Aung, S. S. Shroff, F. T. Arce, R. Lal, G. Arya, S. Varghese, *Biomaterials* **2011**, *32*, 3700.
- [4] C. M. Kelleher, J. P. Vacanti, *J. R. Soc. Interface* **2010**, *7*, S717.
- [5] G. D. Prestwich, *J. Cell. Biochem.* **2007**, *101*, 1370.
- [6] R. C. Dutta, A. K. Dutta, *Biotechnol. Adv.* **2010**, *28*, 764.
- [7] B. A. Justice, N. A. Badr, R. A. Felder, *Drug Discovery Today* **2009**, *14*, 102.
- [8] Z. Melkounian, J. L. Weber, D. M. Weber, A. G. Fadeev, Y. Zhou, P. Dolley-Sonneville, J. Yang, L. Qiu, C. A. Priest, C. Shogbon, A. W. Martin, J. Nelson, P. West, J. P. Beltzer, S. Pal, R. Brandenberger, *Nat. Biotechnol.* **2010**, *28*, 606.
- [9] O. Z. Fisher, A. Khademhosseini, R. Langer, N. A. Peppas, *Acc. Chem. Res.* **2010**, *43*, 419.
- [10] S. R. Van Tomme, G. Storm, W. E. Hennink, *Int. J. Pharm.* **2008**, *355*, 1.
- [11] B. V. Slaughter, S. S. Khurshid, O. Z. Fisher, A. Khademhosseini, N. A. Peppas, *Adv. Mater.* **2009**, *21*, 3307.
- [12] K. Rajagopal, J. P. Schneider, *Curr. Opin. Struct. Biol.* **2004**, *14*, 480.
- [13] X. Zhao, F. Pan, H. Xu, M. Yaseen, H. Shan, C. A. E. Hauser, S. Zhang, J. R. Lu, *Chem. Soc. Rev.* **2010**, *39*, 3480.
- [14] H. Cui, M. J. Webber, S. I. Stupp, *Biopolymers* **2010**, *94*, 1.
- [15] F. Gelain, A. Horii, S. Zhang, *Macromol. Biosci.* **2007**, *7*, 544.
- [16] J. P. Jung, J. Z. Gasiowski, J. H. Collier, *Biopolymers* **2010**, *94*, 49.
- [17] C. A. E. Hauser, S. Zhang, *Chem. Soc. Rev.* **2010**, *39*, 2780.
- [18] S. Cavalli, F. Albericio, A. Kros, *Chem. Soc. Rev.* **2010**, *39*, 241.
- [19] Y. Yang, U. Khoe, X. Wang, A. Horii, H. Yokoi, S. Zhang, *Nano Today* **2009**, *4*, 193.
- [20] S. Zhang, *Nat. Biotechnol.* **2003**, *21*, 1171.
- [21] E. Kokkoli, A. Mardilovich, A. Wedekind, E. L. Rexeis, A. Garg, J. A. Craig, *Soft Matter* **2006**, *2*, 1015.
- [22] S. Kyle, A. Aggeli, E. Ingham, M. J. McPherson, *Trends Biotechnol.* **2009**, *27*, 423.
- [23] S. G. Zhang, T. Holmes, C. Lockshin, A. Rich, *Proc. Natl. Acad. Sci. USA* **1993**, *90*, 3334.
- [24] S. G. Zhang, T. C. Holmes, C. M. Dipersio, R. O. Hynes, X. Su, A. Rich, *Biomaterials* **1995**, *16*, 1385.

- [25] T. C. Holmes, S. de Lacalle, X. Su, G. S. Liu, A. Rich, S. G. Zhang, *Proc. Natl. Acad. Sci. USA* **2000**, 97, 6728.
- [26] A. Horii, X. Wang, F. Gelain, S. Zhang, *PLoS ONE* **2007**, 2, e190.
- [27] H. Misawa, N. Kobayashi, A. Soto-Gutierrez, Y. Chen, A. Yoshida, J. D. Rivas-Carrillo, N. Navarro-Alvarez, K. Tanaka, A. Miki, J. Takei, T. Ueda, M. Tanaka, H. Endo, N. Tanaka, T. Ozaki, *Cell Transplant.* **2006**, 15, 903–910.
- [28] R. G. Ellis-Behnke, Y. X. Liang, S. W. You, D. K. C. Tay, S. G. Zhang, K. F. So, G. E. Schneider, *Proc. Natl. Acad. Sci. USA* **2006**, 103, 5054.
- [29] B. Kao, K. Kadomatsu, Y. Hosaka, *Tissue Eng. Part A* **2009**, 15, 2385.
- [30] Z. Yang, X. Zhao, *Int. J. Nanomedicine* **2011**, 6, 303.
- [31] J. Kisiday, M. Jin, B. Kurz, H. Hung, C. Semino, S. Zhang, A. J. Grodzinsky, *Proc. Natl. Acad. Sci. USA* **2002**, 99, 9996.
- [32] J. Sun, Q. Zheng, Y. Wu, Y. Liu, X. Guo, W. Wu, *J. Huazhong Univ. Sci. Technol. Med. Sci.* **2010**, 30, 173.
- [33] J. Sun, Q. Zheng, Y. Wu, Y. Liu, X. Guo, W. Wu, *Mater. Sci. Eng., C* **2010**, 30, 975.
- [34] A. Aggeli, M. Bell, N. Boden, J. N. Keen, P. F. Knowles, T. C. B. McLeish, M. Pitkeathly, S. E. Radford, *Nature* **1997**, 386, 259.
- [35] A. Aggeli, M. Bell, L. M. Carrick, C. W. G. Fishwick, R. Harding, P. J. Mawer, S. E. Radford, A. E. Strong, N. Boden, *J. Am. Chem. Soc.* **2003**, 125, 9619.
- [36] A. Firth, A. Aggeli, J. L. Burke, X. Yang, J. Kirkham, *Nanomedicine* **2006**, 1, 189.
- [37] J. Kirkham, A. Firth, D. Vernals, N. Boden, C. Robinson, R. C. Shore, S. J. Brookes, A. Aggeli, *J. Dent. Res.* **2007**, 86, 426.
- [38] C. Q. Yan, A. Altunbas, T. Yucel, R. P. Nagarkar, J. P. Schneider, D. J. Pochan, *Soft Matter* **2010**, 6, 5143.
- [39] L. A. Haines-Butterick, D. A. Salick, D. J. Pochan, J. P. Schneider, *Biomaterials* **2008**, 29, 4164.
- [40] L. Haines-Butterick, K. Rajagopal, M. Branco, D. Salick, R. Rughani, M. Pilarz, M. S. Lamm, D. J. Pochan, J. P. Schneider, *Proc. Natl. Acad. Sci. USA* **2007**, 104, 7791.
- [41] E. H. C. Bromley, R. B. Sessions, A. R. Thomson, D. N. Woolfson, *J. Am. Chem. Soc.* **2009**, 131, 928.
- [42] D. Papapostolou, A. M. Smith, E. D. T. Atkins, S. J. Oliver, M. G. Ryadnov, L. C. Serpell, D. N. Woolfson, *Proc. Natl. Acad. Sci. USA* **2007**, 104, 10853.
- [43] M. G. Ryadnov, D. N. Woolfson, *Nat. Mater.* **2003**, 2, 329.
- [44] E. F. Banwell, E. S. Abelardo, D. J. Adams, M. A. Birchall, A. Corrigan, A. M. Donald, M. Kirkland, L. C. Serpell, M. F. Butler, D. N. Woolfson, *Nat. Mater.* **2009**, 8, 596.
- [45] M. Zhou, A. M. Smith, A. K. Das, N. W. Hodson, R. F. Collins, R. V. Ulijn, J. E. Gough, *Biomaterials* **2009**, 30, 2523.
- [46] R. J. Williams, T. E. Hall, V. Glattauer, J. White, P. J. Pasic, A. B. Sorensen, L. Waddington, K. M. McLean, P. D. Currie, P. G. Hartley, *Biomaterials* **2011**, 32, 5304.
- [47] C. A. E. Hauser, R. Deng, A. Mishra, Y. Loo, U. Khoe, F. Zhuang, D. W. Cheong, A. Accardo, M. B. Sullivan, C. Riekel, J. Y. Ying, U. A. Hauser, *Proc. Natl. Acad. Sci. USA* **2011**, 108, 1361.
- [48] A. Mishra, Y. Loo, R. Deng, Y. J. Chuah, H. T. Hee, J. Y. Ying, C. A. E. Hauser, *Nano Today* **2011**, 6, 232.
- [49] J. D. Hartgerink, E. Beniash, S. I. Stupp, *Science* **2001**, 294, 1684.
- [50] H. Hosseinkhani, M. Hosseinkhani, F. Tian, H. Kobayashi, Y. Tabata, *Biomaterials* **2006**, 27, 4079.
- [51] S. Zhang, M. A. Greenfield, A. Mata, L. C. Palmer, R. Bitton, J. R. Mantei, C. Aparicio, M. O. de la Cruz, S. I. Stupp, *Nat. Mater.* **2010**, 9, 594.
- [52] L. T. Lock, E. S. Tzanakakis, *Tissue Eng.* **2007**, 13, 1399.
- [53] E. A. Botchwey, S. R. Pollack, E. M. Levine, C. T. Laurencin, *J. Biomed. Mater. Res.* **2001**, 55, 242.
- [54] J. J. Schmidt, J. Jeong, H. Kong, *Tissue Eng. Part A* **2011**, 17, 2687.
- [55] B. Zamanian, M. Masaeli, J. W. Nichol, M. Khabiry, M. J. Hancock, H. Bae, A. Khademhosseini, *Small* **2010**, 6, 937.
- [56] Y. Tsuda, Y. Morimoto, S. Takeuchi, *Langmuir* **2009**, 26, 2645.
- [57] Y. F. Tian, J. M. Devgun, J. H. Collier, *Soft Matter* **2011**, 7, 6005.
- [58] D. I. Rozkiewicz, B. D. Myers, S. I. Stupp, *Angew. Chem., Int. Ed.* **2011**, 50, 6324.
- [59] I. Wheeldon, A. Farhadi, A. G. Bick, E. Jabbari, A. Khademhosseini, *Nanotechnology* **2011**, 22, 212001.
- [60] G. A. Silva, C. Czeisler, K. L. Niece, E. Beniash, D. A. Harrington, J. A. Kessler, S. I. Stupp, *Science* **2004**, 303, 1352.
- [61] R. N. Shah, N. A. Shah, M. M. D. R. Lim, C. Hsieh, G. Nuber, S. I. Stupp, *Proc. Natl. Acad. Sci. USA* **2010**, 107, 3293.
- [62] A. Mata, Y. Geng, K. J. Henrikson, C. Aparicio, S. R. Stock, R. L. Satcher, S. I. Stupp, *Biomaterials* **2010**, 31, 6004.
- [63] F. Gelain, D. Bottai, A. Vescovi, S. Zhang, *PLoS ONE* **2006**, 1, e119.
- [64] F. Gelain, D. Silva, A. Caprini, F. Taraballi, A. Natalello, O. Villa, K. T. Nam, R. N. Zuckermann, S. M. Doglia, A. Vescovi, *ACS Nano* **2011**, 5, 1845.
- [65] Z. X. Zhang, Q. X. Zheng, Y. C. Wu, D. J. Hao, *Biotechnol. Bioprocess Eng.* **2010**, 15, 545.
- [66] Y. Kumada, S. G. Zhang, *PLoS ONE* **2010**, 5, e10305.
- [67] F. Gelain, L. D. Unsworth, S. Zhang, *J. Controlled Release* **2010**, 145, 231.
- [68] M. E. Davis, P. C. H. Hsieh, T. Takahashi, Q. Song, S. G. Zhang, R. D. Kamm, A. J. Grodzinsky, P. Anversa, R. T. Lee, *Proc. Natl. Acad. Sci. USA* **2006**, 103, 8155.
- [69] J. H. Kim, Y. Jung, S.-H. Kim, K. Sun, J. Choi, H. C. Kim, Y. Park, S. H. Kim, *Biomaterials* **2011**, 32, 6080.
- [70] L. W. Chow, R. Bitton, M. J. Webber, D. Carvajal, K. R. Shull, A. K. Sharma, S. I. Stupp, *Biomaterials* **2011**, 32, 1574.
- [71] P. Menasche, *Curr. Opin. Cardiol.* **2004**, 19, 154.
- [72] L. W. Chow, L. J. Wang, D. B. Kaufman, S. I. Stupp, *Biomaterials* **2010**, 31, 6154.
- [73] K. Rajangam, M. S. Arnold, M. A. Rocco, S. I. Stupp, *Biomaterials* **2008**, 29, 3298.
- [74] S. Ghanaati, M. J. Webber, R. E. Unger, C. Orth, J. F. Hulvat, S. E. Kiehna, M. Barbeck, A. Rasic, S. I. Stupp, C. J. Kirkpatrick, *Biomaterials* **2009**, 30, 6202.
- [75] P. W. Kopesky, E. J. Vanderploeg, J. D. Kisiday, D. D. Frisbie, N. D. Sandy, A. J. Grodzinsky, *Tissue Eng. Part A* **2011**, 17, 83.
- [76] N. L. Angeloni, C. W. Bond, Y. Tang, D. A. Harrington, S. Zhang, S. I. Stupp, K. E. McKenna, C. A. Podlasek, *Biomaterials* **2011**, 32, 1091.
- [77] H. W. Jun, V. Yuwono, S. E. Paramonov, J. D. Hartgerink, *Adv. Mater.* **2005**, 17, 2612.
- [78] Y. Chau, Y. Luo, A. C. Y. Cheung, Y. Nagai, S. Zhang, J. B. Kobler, S. M. Zeitels, R. Langer, *Biomaterials* **2008**, 29, 1713.
- [79] Y. Kumada, N. A. Hammond, S. G. Zhang, *Soft Matter* **2010**, 6, 5073.
- [80] K. M. Galler, L. Aulisa, K. R. Regan, R. N. D'Souza, J. D. Hartgerink, *J. Am. Chem. Soc.* **2010**, 132, 3217.
- [81] E. L. Bakota, Y. Wang, F. R. Danesh, J. D. Hartgerink, *Biomacromolecules* **2011**, 12, 1651.
- [82] K. M. Galler, A. Cavender, V. Yuwono, H. Dong, S. Shi, G. Schmalz, J. D. Hartgerink, R. N. D'Souza, *Tissue Eng. Part A* **2008**, 14, 2051.
- [83] M. C. Giano, D. J. Pochan, J. P. Schneider, *Biomaterials* **2011**, 32, 6471.



- [84] T. D. Sargeant, M. O. Guler, S. M. Oppenheimer, A. Mata, R. L. Satcher, D. C. Dunand, S. I. Stupp, *Biomaterials* **2008**, 29, 161.
- [85] Y. Wang, L. Zhao, B. M. Hantash, *Biomaterials* **2010**, 31, 5122.
- [86] L. C. Wu, J. Yang, J. Kopecek, *Biomaterials* **2011**, 32, 5341.
- [87] A. Andukuri, M. Kushwaha, A. Tambralli, J. M. Anderson, D. R. Dean, J. L. Berry, Y. D. Sohn, Y.-S. Yoon, B. C. Brott, H.-W. Jun, *Acta Biomater.* **2011**, 7, 225.
- [88] D. M. Elzey, H. N. G. Wadley, *Acta Mater.* **2001**, 49, 849.
- [89] P. Brun, F. Ghezzi, M. Roso, R. Danesin, G. Palu, A. Bagno, M. Modesti, I. Castagliuolo, M. Dettin, *Acta Biomater.* **2011**, 7, 2526.
- [90] V. Beachley, X. Wen, *Prog. Polym. Sci.* **2010**, 35, 868.
- [91] Z. Mahmoud, D. Grudy, K. Channon, D. Woolfson, *Biomaterials* **2010**, 31, 7468.
- [92] Z. Mahmoud, S. Gunnoo, A. Thomson, J. Fletcher, D. Woolfson, *Biomaterials* **2011**, 32, 3712.
- [93] M. Ikeda, T. Tanida, T. Yoshii, I. Hamachi, *Adv. Mater.* **2011**, 23, 2819.
- [94] S. Fung, H. Yang, P. Sadatmousavi, Y. Sheng, T. Marno, R. Nazarian, P. Chen, *Adv. Funct. Mater.* **2011**, 21, 2456.
- [95] S. Kyle, A. Aggeli, E. Ingham, M. J. McPherson, *Biomaterials* **2010**, 31, 9395.